

Changes in Apparent Free Energy of Helix–Helix Dimerization in a Biological Membrane Due to Point Mutations

Mylinh T. Duong¹, Todd M. Jaszewski¹, Karen G. Fleming²
and Kevin R. MacKenzie^{1*}

¹Department of Biochemistry
and Cell Biology
Rice University, Houston
TX 77005, USA

²T.C. Jenkins Department of
Biophysics, Johns Hopkins
University, Baltimore
MD 21218, USA

We present an implementation of the TOXCAT membrane protein self-association assay that measures the change in apparent free energy of transmembrane helix dimerization caused by point mutations. Quantifying the reporter gene expression from cells carrying wild-type and mutant constructs shows that single point mutations that disrupt dimerization of the transmembrane domain of glycoporphin A reproducibly lower the TOXCAT signal more than 100-fold. Replicate cultures can show up to threefold changes in the level of expression of the membrane bound fusion construct, and correcting for these variations improves the precision of the calculated apparent free energy change. The remarkably good agreement between our TOXCAT apparent free energy scale and free energy differences from sedimentation equilibrium studies for point mutants of the glycoporphin A transmembrane domain dimer indicate that sequence changes usually affect membrane helix–helix interactions quite similarly in these two very different environments. However, the effects of point mutations at threonine 87 suggest that intermonomer polar contacts by this side-chain contribute significantly to dimer stability in membranes but not in detergents. Our findings demonstrate that a comparison of quantitative measurements of helix–helix interactions in biological membranes and genuine thermodynamic data from biophysical measurements on purified proteins can elucidate how changes in the lipidic environment modulate membrane protein stability.

© 2007 Elsevier Ltd. All rights reserved.

Keywords: dimerization; glycoporphin A; transmembrane domain; thermodynamics; TOXCAT

*Corresponding author

Introduction

Lateral interactions between transmembrane helices are important determinants of the folding and stability of α -helical integral membrane proteins and can provide a significant driving force for oligomerization of single-spanning proteins.¹ Biochemical and biophysical methods have provided measures of the stability of transmembrane domain (TMD) oligomers in detergents^{2–5} and in synthetic

membranes,^{6,7} and studies with sequence variants have revealed how amino acid sequence can influence transmembrane helix–helix interactions.^{8–11} These *in vitro* approaches have been complemented by the development of cell-based assays for TMD interactions within biological membranes.^{12–17} In these biological assays, membrane spanning domains of interest are fused to oligomerization-dependent DNA binding domains and the expressed chimeric proteins are localized to the inner membrane of *Escherichia coli* with their DNA binding domains in the cytosol. Association of the TMDs brings the DNA binding domains into close proximity, allowing them to bind to a target regulatory DNA sequence and thereby modulate transcription of a reporter gene. The extent of transmembrane helix–helix interaction can be inferred from the level of reporter gene ex-

Abbreviations used: TMD, transmembrane domain; CAT, chloramphenicol acetyl transferase; MBP, maltose binding protein.

E-mail address of the corresponding author:
mev@rice.edu

pression; in some assays, association causes transcriptional activation,^{12,14} whereas in others it causes repression.^{15,17}

A rank order of association propensity for different membrane spans can be established with any of these assays, and site-directed mutagenesis has been used in combination with several different biological assays for transmembrane helix association to identify residues that are critical to helix–helix interactions of natural^{12,13,18–30} and designed^{31,32} membrane spans. Sequences that have been shown to associate tightly and specifically, such as glycophorin A,^{33,34} usually serve as positive controls in these experiments. The qualitative conclusions drawn from these data about the propensity of TMDs to interact can be contrasted with the quantitative thermodynamic information obtained from biophysical approaches to measuring interactions between membrane proteins. In particular, sedimentation equilibrium ultracentrifugation has been used to measure free energies of association for many different membrane protein systems, and a few studies have probed the sequence dependence of helix–helix association in considerable detail,^{9–11} allowing the relationship between membrane protein structure and stability to be explored quantitatively. However, because these measurements are performed on proteins in a detergent micelle environment, the relevance of these data to the behavior of the same proteins in native membranes is not clear.

The well-studied transmembrane span of glycophorin A provides an excellent system in which to compare the stability and sequence specificity of TMD interactions in different lipidic environments. The sequence dependence of glycophorin A TMD dimerization was first examined by a saturation mutagenesis approach using an SDS-PAGE assay,^{33,34} and a systematic set of interfacial substitutions have been studied by sedimentation equilibrium analytical ultracentrifugation.^{2,8–10,35} The ToxR^{12,13} and TOXCAT¹⁴ biological assays have been used to examine both wild-type glycophorin A and a number of mutants, and the rank order of stability of mutants analyzed by biophysical and biological approaches agrees well.⁸ Here, we examine 28 point mutants of the glycophorin A transmembrane domain using the TOXCAT assay with the goal of quantitatively assessing the effects of point mutations on dimerization of the membrane span *in vivo*. We describe an implementation of TOXCAT that enables us to determine the apparent change in the free energy of dimerization due to mutations ($\Delta\Delta G_{app}$). We find generally good agreement between these biological $\Delta\Delta G_{app}$ values and previously reported $\Delta\Delta G_{mut}$ values for these mutations from sedimentation equilibrium in detergents. Outliers suggest that polar interactions of the side-chain γ oxygen of threonine 87 of glycophorin A are important to TMD dimer stability in bilayers but not in detergents.

Theory and assumptions

TOXCAT is a biological assay in which expression of the reporter gene chloramphenicol acetyltransferase (CAT) is driven by oligomerization-dependent transcriptional activation by a membrane-inserted fusion protein¹⁴ (see Figure 1). We seek to express the association constant describing dimerization of the TOXCAT fusion protein in terms of readily measurable parameters. Assuming that the fusion protein is present in the cell membrane only as monomers or dimers, the oligomerization reaction of the fusion protein and the corresponding equilibrium association constant K_a are given by:

$$P + P \leftrightarrow P_2 \quad K_a = [P_2]/[P]^2 \quad (1)$$

where $[P]$ represents the mole fraction of monomeric fusion protein (relative to moles of all lipids and proteins in the membrane), $[P_2]$ represents the mole fraction of dimeric fusion protein, and the mole fraction of total protein, $[P_{total}]$, is given by:

$$[P_{total}] = [P] + 2[P_2] \quad (2)$$

and so:

$$K_a = [P_2]/([P_{total}] - 2[P_2])^2 \quad (3)$$

In the limit where $[P_2]$ is small we can make the approximation:

$$[P] \approx [P_{total}] \quad (4)$$

which simplifies the expression for the apparent equilibrium constant to:

$$K_{app} = [P_2]/[P_{total}]^2 \quad (5)$$

This expression for K_{app} can be related to measurable parameters from the TOXCAT assay. We assume that the mole fraction of dimeric TOXCAT fusion protein, $[P_2]$, is given by the expression level of the reporter gene, $CAT_{lystate}$, times a proportionality constant α :

$$[P_2] = \alpha \times CAT_{lystate} \quad (6)$$

and that the mole fraction of total TOXCAT fusion protein, $[P_{total}]$, is given by the Western blot band intensity of a standardized amount of membrane, $WB_{lystate}$, times a proportionality constant β that

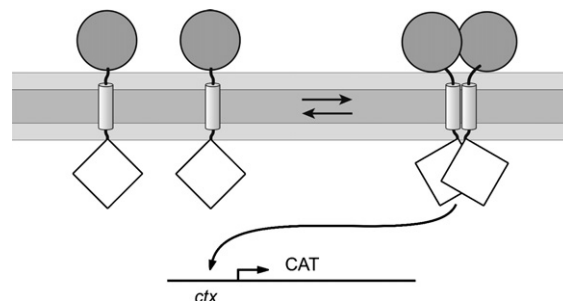


Figure 1. Schematic representation of the TOXCAT assay.¹⁴ ToxR' domains (diamonds) can activate transcription of the reporter gene (CAT) if brought together by the transmembrane domains. The maltose binding protein domain (circles) helps direct the insertion of the construct into the membrane, complements the *malE* mutation in the host cells, and serves as an epitope for quantifying the level of fusion protein.

includes the moles of total lipid and protein in the membrane aliquot:

$$[P_{\text{total}}] = \beta \times WB_{\text{lysate}} \quad (7)$$

To determine the absolute K_{app} (and thus the apparent free energy of association, ΔG_{app}), we would need the proportionality constants α and β . However, when we write an expression for the ratio of the apparent association constants for wild-type and mutant TMDs:

$$\frac{K_{\text{app}}^{\text{mut}}}{K_{\text{app}}^{\text{WT}}} = \frac{[P_2^{\text{mut}}] [P_{\text{total}}^{\text{WT}}]^2}{[P_2^{\text{WT}}] [P_{\text{total}}^{\text{mut}}]^2} = \frac{\alpha \text{CAT}_{\text{mut}} (\beta WB_{\text{WT}})^2}{(\beta WB_{\text{mut}})^2 \alpha \text{CAT}_{\text{WT}}} \quad (8)$$

we can rearrange the terms, cancel the proportionality constants, and calculate $\Delta \Delta G_{\text{app}}$, the apparent change in free energy of association that results from a mutation to the TMD sequence, using the expression:

$$\Delta \Delta G_{\text{app}} = -RT \ln (\text{CAT}_{\text{mut}}/\text{CAT}_{\text{WT}})(WB_{\text{WT}}/WB_{\text{mut}})^2 \quad (9)$$

where the term $\text{CAT}_{\text{mut}}/\text{CAT}_{\text{WT}}$ is the ratio of CAT activity from normalized amounts of cells expressing mutant or wild-type constructs, and the term $WB_{\text{WT}}/WB_{\text{mut}}$ is the ratio of the band intensities for wild-type or mutant TOXCAT fusion proteins on a Western blot of normalized amounts of cells.

This approach will begin to break down when a substantial fraction of the fusion protein in the membrane forms dimers, so that the amount of monomeric protein can no longer be approximated as the total amount of protein. Analysis of our data indicates that the assumption of a small fraction of dimer does not significantly bias our TOXCAT results and that the simplification that we employ permits us to extract useful information about the sequence dependence of the stability of helix–helix interactions inside membranes of living cells.

Results

Wild-type and mutant glycoporphin A TOXCAT fusion proteins insert into the *E. coli* inner membrane with the appropriate topology

We explored the effects of single point mutations on the TOXCAT *in vivo* dimerization signal for the transmembrane domain of glycoporphin A by altering the TMD sequence of the ToxR'(GpA-TMD)MBP construct described by Russ and Engelman.¹⁴ We generated the library of single point mutants of glycoporphin A previously studied by Fleming and colleagues *in vitro* using sedimentation equilibrium analytical ultracentrifugation,^{2,8–10,35} most of these had previously been characterized under conditions of SDS-PAGE.^{33,36} After transformation of these TOXCAT constructs into *Escherichia coli* NT326 cells, we tested the ability of the wild-type and mutant fusion proteins to complement the *malE* phenotype of

the NT326 strain by growing each construct on plates containing maltose as the sole carbon source. Cells containing constructs that lack a TMD do not grow, but the wild-type ToxR'(GpA-TMD)MBP construct and all point mutants support robust growth on maltose (Figure 2), indicating that the MBP domains of these fusion proteins are being targeted to the periplasm of the NT326 cells. We conclude that the expected topology (see Figure 1) is being achieved by these proteins, in agreement with previous reports for wild-type glycoporphin A and point mutants in the ToxR^{12,13} and TOXCAT¹⁴ assays.

Mutations can modulate the glycoporphin A TOXCAT signal by a factor of 200

We quantified the TOXCAT dimerization signal using the spectrophotometric CAT assay³⁷ that we had previously applied in studies of BNIP3 TMD dimerization.³⁸ The colorimetric assay has poorer absolute sensitivity than assays based on radioactive³⁹ or fluorescent⁴⁰ substrates employed for quantifying CAT activity, but the signal can be measured quickly and with high precision because the data correspond to the slope of a straight line from a least-squares fit to 20 or 40 absorption measurements over 1 or 2 min in the same cuvette. Standard errors in triplicate assays of a lysate having high levels of CAT activity are at the limit of pipetting precision, while at low levels of CAT activity, the error between repeats is about 0.1 unit. NT326 cells expressing wild-type ToxR'(GpA-TMD)MBP constructs give lysates that contain 190–200 units of CAT, while cells carrying certain point mutants in the GpA-TMD give lysates that

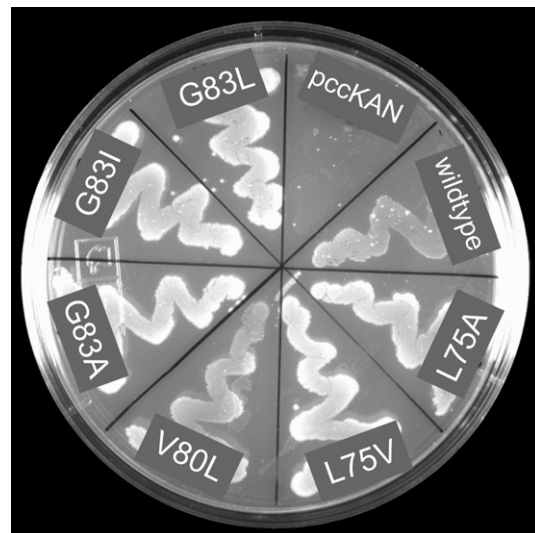


Figure 2. Complementation assays for wild-type and selected mutant glycoporphin A ToxR' fusion constructs. NT326 cells (*malE*) carrying various constructs were streaked on a plate with maltose as the sole carbon source and grown for three days at 37 °C. All ToxR'(GpA-TMD)MBP fusion constructs permit robust growth of NT326 cells on maltose, while control transformants (*pccKAN*) do not.

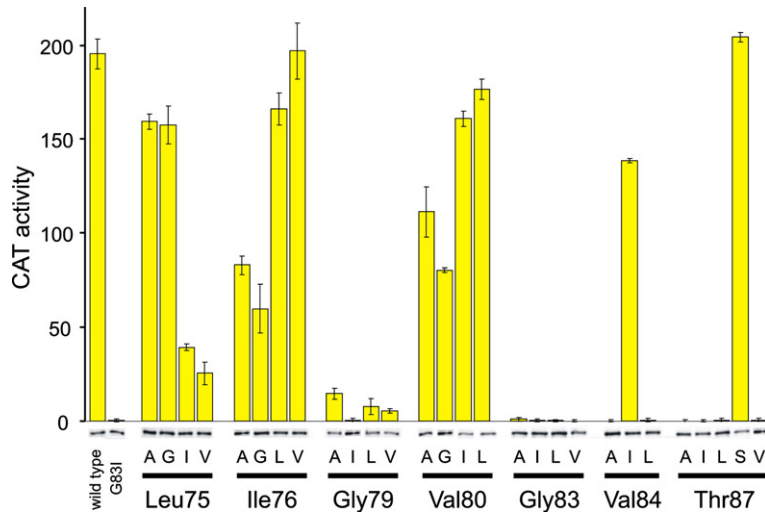


Figure 3. Reporter gene activity and fusion construct expression data for one replicate of mutant and wild-type glycoporphin A constructs. Yellow bars represent the CAT activity quantified from cleared lysates, and error bars represent the standard error for three measurements of each lysate. Bands below the bars are details from Western blots of the ToxR fusions; the intensities of these bands were quantified by photon counting of chemiluminescence. The differences in the observed CAT activity are much larger than the differences in ToxR fusion expression level.

contain 0.2–0.5 units of CAT (see Figure 3). These differences in TOXCAT signal are reproduced across independent cultures (see columns in Table 1). The ability to accurately and precisely measure the level of expressed CAT is essential to our approach, and we note that the amount of cells harvested to prepare the lysates was optimized to improve the lower detection limit of the assay.

Expression levels of the TOXCAT fusion protein vary significantly from culture to culture

Differences in the TOXCAT signals of two cultures can arise from differences in the self-association of the membrane-inserted fusion proteins but may also reflect variations in the total amounts of fusion protein expressed. To control for this possibility,

Table 1. Terms contributing to the apparent free energy change of glycoporphin A dimerization

Seq	$-RT \ln [CAT_{mut}/CAT_{WT}]$ (kcal mol ⁻¹)				$-RT \ln [WB_{WT}/WB_{mut}]^2$ (kcal mol ⁻¹)				$\Delta\Delta G_{app}$ (kcal mol ⁻¹)					SD _{CAT} ⁺ SD _{WB}
	1	2	3	SD _{CAT}	1	2	3	SD _{WB}	1	2	3	Mean	SD _{ΔΔG}	
L75A	0.70	0.48	0.46	0.13	0.21	-0.16	-0.02	0.19	0.91	0.32	0.44	0.56	0.31	0.32
L75G	0.08	0.06	0.14	0.04	0.37	0.27	0.29	0.05	0.45	0.33	0.43	0.41	0.07	0.10
L75I	1.40	1.13	1.05	0.18	-0.11	0.49	0.21	0.30	1.29	1.62	1.26	1.39	0.20	0.48
L75V	1.53	1.11	1.33	0.21	0.06	1.00	0.18	0.51	1.59	2.11	1.52	1.74	0.32	0.72 ^a
I76A	0.68	0.83	0.65	0.09	-0.10	-0.17	-0.31	0.11	0.57	0.66	0.34	0.52	0.16	0.20
I76G	1.11	0.56	0.78	0.28	0.27	0.73	0.36	0.24	1.38	1.30	1.14	1.27	0.13	0.52 ^a
I76L	0.08	0.06	0.55	0.28	0.47	0.64	0.01	0.33	0.55	0.71	0.57	0.61	0.09	0.61 ^a
I76V	0.29	-0.07	-0.01	0.19	0.56	0.46	0.03	0.28	0.85	0.39	0.03	0.42	0.41	0.47
G79A	1.95	1.45	1.70	0.25	0.15	0.42	-0.42	0.43	2.10	1.88	1.28	1.75	0.42	0.68
G79I	4.17	5.08	4.63	0.45	-0.09	-0.08	0.13	0.12	4.08	5.00	4.75	4.61	0.47	0.58
G79L	2.23	1.93	2.35	0.22	0.71	0.87	0.02	0.46	2.94	2.80	2.37	2.70	0.30	0.67 ^a
G79V	2.44	1.91	2.66	0.39	-0.04	1.04	-0.43	0.76	2.40	2.95	2.23	2.53	0.37	1.15 ^b
V80A	0.51	0.01	0.37	0.25	0.06	1.15	-0.16	0.70	0.57	1.16	0.21	0.64	0.48	0.95 ^a
V80G	0.70	0.71	0.74	0.03	-0.21	-0.18	-0.45	0.15	0.49	0.53	0.29	0.44	0.13	0.17
V80I	0.45	0.10	0.13	0.19	0.24	-0.13	0.11	0.19	0.69	-0.03	0.24	0.30	0.36	0.38
V80L	0.16	0.14	0.08	0.04	0.11	0.45	-0.10	0.28	0.27	0.59	-0.01	0.28	0.30	0.32
G83A	3.25	3.27	3.48	0.13	0.55	0.69	0.52	0.09	3.80	3.97	4.00	3.92	0.11	0.22
G83I	4.76	4.01	4.53	0.39	0.54	0.82	0.68	0.14	5.30	4.83	5.21	5.11	0.25	0.53
G83L	4.31	3.86	4.44	0.30	0.19	0.82	0.84	0.37	4.50	4.68	5.28	4.82	0.41	0.68
G83V	3.71	3.86	3.26	0.31	0.01	-0.07	-0.09	0.05	3.72	3.79	3.17	3.56	0.34	0.36
V84A	3.05	3.39	4.53	0.78	0.04	0.05	-1.11	0.67	3.09	3.44	3.42	3.32	0.20	1.44 ^b
V84I	0.24	0.28	0.24	0.02	-0.16	0.37	0.52	0.36	0.08	0.65	0.76	0.50	0.37	0.38
V84L	3.38	3.23	2.62	0.41	0.42	0.37	0.09	0.18	3.80	3.60	2.70	3.37	0.58	0.58
T87A	2.93	3.73	4.99	1.03	0.45	0.34	-1.00	0.81	3.38	4.07	3.99	3.81	0.37	1.84 ^b
T87I	4.31	3.73	4.53	0.42	0.10	0.32	-0.39	0.36	4.40	4.05	4.14	4.20	0.18	0.78 ^b
T87L	3.46	3.99	3.32	0.36	0.04	0.02	0.54	0.30	3.50	4.01	3.86	3.79	0.26	0.65 ^a
T87S	-0.12	0.03	-0.01	0.08	0.30	0.03	0.50	0.23	0.18	0.07	0.49	0.25	0.22	0.31
T87V	4.36	4.17	5.08	0.48	-0.58	-0.28	-0.74	0.24	3.78	3.89	4.34	4.01	0.29	0.72 ^a
! Avg				0.28				0.32					0.29	0.60 ^a

SD_{CAT}, SD_{WB}: standard deviation of the CAT term, $-RT \ln [CAT_{mut}/CAT_{WT}]$, and the WB term, $-RT \ln [WB_{WT}/WB_{mut}]$, for the three independent cultures.

SD_{ΔΔG}: standard deviation of $\Delta\Delta G_{app}$ from three independent cultures.

^a Sum of the standard errors of the CAT and WB terms exceeds the standard error of $\Delta\Delta G_{app}$ by 0.30 kcal mol⁻¹ or more.

^b Sum of the standard errors of the CAT and WB terms exceeds the standard error of $\Delta\Delta G_{app}$ by 0.60 kcal mol⁻¹ or more.

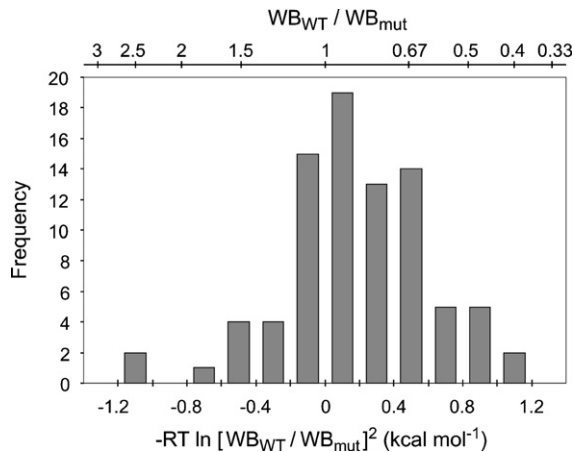


Figure 4. Histogram of the variation in ToxR'(GpA-TMD)MBP fusion expression compared to wild-type. The top scale gives the ratio of wild-type to mutant Western blot band intensity; the bottom scale converts this ratio to the term used to correct the apparent free energy. Each of the 84 mutant cultures is represented in this Figure, scaled to the wild-type culture with which it was grown on that particular day. The level of expression of the fusion construct can affect the apparent free energy by as much as 1 kcal mol⁻¹ in either direction.

each culture assayed for CAT activity was also assayed to determine the relative levels of full-length fusion construct present. Whole cell lysates from cells expressing wild-type and mutant constructs were separated by SDS-PAGE and protein levels were quantified in Western blots using an anti-MBP primary antibody. NT326 cultures carrying ToxR'(GpA-TMD)MBP mutants expressed slightly more protein (115%) than wild-type on average, and the distribution of protein levels was quite broad (see Figure 4), with cultures exhibiting as little as 40% or as much as 260% of wild-type fusion protein expression. A total of 50 of the 84 cultures (60%) showed between 85% and 150% of wild type fusion protein levels, whereas 72 of the 84 cultures (86%) expressed between 67% and 200% of wild-type levels. Certain constructs (Thr87Val, Gly83Ala) reproducibly under or over-expressed relative to wild-type, but variation in expression can be independent of the sequence of the mutant TMD: in two instances (Val84Ala and Gly79Val), cultures grown from the same glycerol stock on different days gave lysates whose expression level of fusion protein varied more than threefold relative to wild-type cultures grown on those same days. These differences can be expected to have strong effects on the amount of dimerization signal (CAT activity) seen in these cells.

CAT activity and fusion protein levels can be combined to give precise values for $\Delta\Delta G_{app}$

To show how both CAT activity and the level of TOXCAT fusion protein impact the calculation of

$\Delta\Delta G_{app}$, we separate the logarithm in equation (9) to give:

$$\Delta\Delta G_{app} = -RT \ln (CAT_{mut}/CAT_{WT}) - RT \ln (WB_{WT}/WB_{mut})^2 \quad (10)$$

and report $-RT \ln (CAT_{mut}/CAT_{WT})$ and $-RT \ln (WB_{WT}/WB_{mut})^2$ in units of kcal mol⁻¹ for each culture studied (see Table 1). The term based on CAT activities ranges from -0.12 to $+5.08$ kcal mol⁻¹, indicating that the CAT data can report on very significant disruption of transmembrane domain dimerization. The term based on Western blot intensities ranges from -1.11 to $+1.15$ kcal mol⁻¹, showing that the measured level of TOXCAT protein can contribute appreciably, in either direction, to the final value of $\Delta\Delta G_{app}$. We observe a much larger range of raw CAT values than blot values, but because our derivation treats fusion protein interaction as a bimolecular association, the squaring of the blot ratio doubles the impact of the differences in blot intensities. Based only on the magnitudes of the CAT and blot terms, it would appear that both can be important to calculating $\Delta\Delta G_{app}$.

For many mutants, each of the terms in equation (10) clusters closely for the three independent cultures: as seen in Table 1 for Gly83Ala, the CAT-based terms are 3.25, 3.27, and 3.48 kcal mol⁻¹ (standard deviation=0.13 kcal mol⁻¹) and the blot-based terms are 0.55, 0.69, and 0.52 kcal mol⁻¹ (standard deviation=0.09 kcal mol⁻¹). Although this particular example is among the best in the dataset, the average standard deviations for the CAT-based terms and the blot-based terms for the 28 mutants in Table 1 are 0.28 and 0.32 kcal mol⁻¹, respectively, demonstrating that our experimental protocol is usually highly reproducible. In some instances, however, the three independent cultures show large differences in the measured parameters. Mutant Val84Ala has CAT-based terms of 3.05, 3.39, and 4.53 kcal mol⁻¹ (mean=3.66, standard deviation=0.78 kcal mol⁻¹) and blot-based terms of 0.04, 0.05, and -1.11 kcal mol⁻¹ (mean= -0.34 , standard deviation=0.67 kcal mol⁻¹). Summing these averages gives $\Delta\Delta G_{app}=3.32$ kcal mol⁻¹ with a standard deviation of 1.45 kcal mol⁻¹, which initially suggests that $\Delta\Delta G_{app}$ is much less reliable for this particular mutant than for others. However, if the CAT-based and blot-based terms for each independent culture are first added together, the independently determined values for $\Delta\Delta G_{app}$ are 3.09, 3.44, and 3.42 kcal mol⁻¹ (mean=3.32, standard deviation=0.20 kcal mol⁻¹), which indicates that this mutant also shows good reproducibility. This demonstrates that the CAT and Western blot values are correlated, and suggests that our blot-based term compensates for variations in the fusion protein expression level that affect the CAT activity measured in cell lysates. This compensation is observed over the entire data set: Table 1 shows that the average standard deviation of the independently determined values

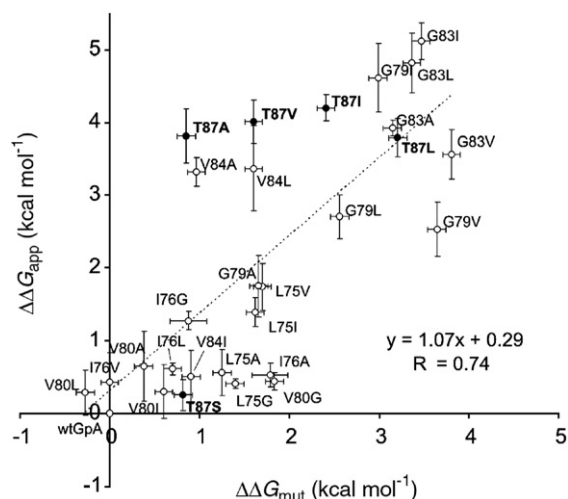


Figure 5. Correlation of TOXCAT apparent free energy changes with free energy differences determined by sedimentation equilibrium analytical ultracentrifugation.^{2,8–10,35} Mutations involving Thr87 are represented as black dots and are labeled in bold; omitting these data points from the fit gives $R=0.80$. The near-unity slope of this fit shows that the TOXCAT assay samples the same range as the biophysical measurements.

for $\Delta\Delta G_{\text{app}}$ is $0.29 \text{ kcal mol}^{-1}$, whereas the sum of the average standard deviations of the CAT and Western blot terms is $0.60 \text{ kcal mol}^{-1}$. Mutants for which the sum of the standard deviations of the CAT and Western blot terms exceeds the standard deviation of $\Delta\Delta G_{\text{app}}$ by at least 0.30 (or 0.60) kcal mol^{-1} are identified by superscripts in the last column of Table 1. It is also noteworthy that the standard deviation of $\Delta\Delta G_{\text{app}}$ does not exceed the sum of the CAT and Western blot standard deviations for any of the 28 mutants, as might occur by chance even if the variances of the two terms were merely uncorrelated.

$\Delta\Delta G_{\text{app}}$ corresponds closely to $\Delta\Delta G_{\text{mut}}$ from ultracentrifugation

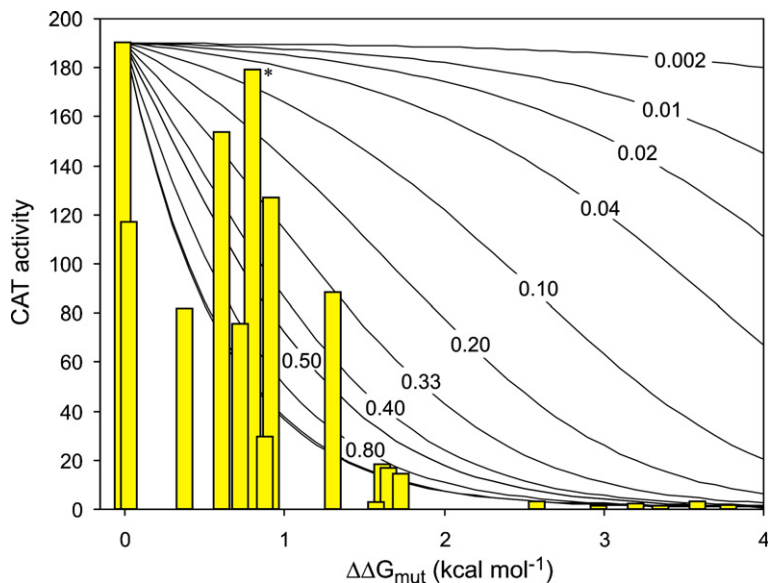
We compared our set of $\Delta\Delta G_{\text{app}}$ values for point mutants of the glycoporphin A TMD with the thermodynamic data of Fleming and colleagues^{2,8–10} for which the free energy change of dimerization associated with a mutation, $\Delta\Delta G_{\text{mut}}$, has been determined by measuring the free energy of association of both wild-type and mutant fusion proteins in detergent micelles by sedimentation equilibrium analytical ultracentrifugation. Using Student's *t*-test, only eight of 28 mutants (Leu75Gly, Ile76Ala, Val80Gly, Gly83Ile, Val84Ala, Thr87Ala, Thr87Ile, and Thr87Val) show values of $\Delta\Delta G_{\text{app}}$ that differ significantly from $\Delta\Delta G_{\text{mut}}$ (at the 95% confidence level; see Experimental Methods). This could simply mean that the *t*-test fails to find significant differences because the data have large standard deviations. However, the same *t*-test criteria show that 18 of the 28 values for $\Delta\Delta G_{\text{app}}$ differ significantly from

no change in stability ($0.0 (\pm 0.1) \text{ kcal mol}^{-1}$), another set of 18 values for $\Delta\Delta G_{\text{app}}$ differ significantly from the most disruptive $\Delta\Delta G_{\text{mut}}$ ($3.8 (\pm 0.1) \text{ kcal mol}^{-1}$), and 17 values for $\Delta\Delta G_{\text{app}}$ differ significantly from an intermediate value of $1.9 (\pm 0.1) \text{ kcal mol}^{-1}$. Thus, the range and standard deviations of $\Delta\Delta G_{\text{app}}$ do allow the *t*-test to distinguish among the range of values of $\Delta\Delta G_{\text{mut}}$. We conclude that the measured values of $\Delta\Delta G_{\text{app}}$ are broadly distributed for the different mutants and that the majority of these values correspond closely to the independently determined values of $\Delta\Delta G_{\text{mut}}$.

Regression analysis of $\Delta\Delta G_{\text{app}}$ versus $\Delta\Delta G_{\text{mut}}$ for all 28 mutants yields a fit with a slope of 1.07 and a correlation coefficient $R=0.74$ (Figure 5); note that the error bars in Figure 5 represent the standard errors for three independent ultracentrifuge experiments (for $\Delta\Delta G_{\text{mut}}$) or the standard errors for three independent TOXCAT cultures (for $\Delta\Delta G_{\text{app}}$). Omitting the five mutants at position Thr87 (for reasons presented in the Discussion) improves the fit ($R=0.80$, slope=1.08, intercept=0.06). Together, the *t*-tests and regression analyses indicate that the effects of individual point mutations on glycoporphin A dimerization as assessed *in vivo* using TOXCAT are usually similar to the effects seen by analytical ultracentrifugation of purified proteins in detergent. These findings suggest that the two methods are measuring the same basic phenomena despite the differences between the contexts in which the measurements are made. By contrast, statistically significant differences between $\Delta\Delta G_{\text{app}}$ and $\Delta\Delta G_{\text{mut}}$ for certain mutants suggest that the association tendencies of these particular glycoporphin A variants are not the same in detergents and in TOXCAT.

Evaluating the assumption that the fusion protein is largely monomeric

Although our method does not directly determine the mole fraction of monomer and dimer for any of our ToxR fusions, the wide range of observed CAT activities for different mutants and the corresponding values from ultracentrifugation for $\Delta\Delta G_{\text{mut}}$ allow us to make inferences about the fractional association of the wild-type fusion protein. If the wild-type ToxR'(GpA-TMD)MBP fusion protein were present at high mole fraction and thus existed primarily as dimers in *E. coli* membranes, then slightly destabilizing mutations ($+1.0 \text{ kcal mol}^{-1}$) would be expected to cause little change in the mole fraction of dimeric protein or in the observed CAT activity. We simulated the effects of perturbing the free energy of dimerization assuming that different initial levels of association for the wild-type protein were giving rise to wild-type levels of CAT activity (see Figure 6). Essentially no change in observed CAT signal would be expected if an overwhelmingly dimeric wild-type construct (fraction monomer=0.002, corresponding to the regime where $[P_{\text{total}}] \gg 1/K_a$) were destabilized by up to 4 kcal mol^{-1} . By comparing the



brium.^{2,8–10,35} Outliers from the *t*-test comparison have been excluded. CAT activities shown are for individual replicates with very similar fusion protein expression levels, eliminating the need to correct for concentration effects. The yellow bar labeled with an asterisk corresponds to Thr87Ser, which is mildly disruptive by sedimentation equilibrium but dimerizes as wild-type in TOXCAT.

theoretical lines in Figure 6 to raw CAT data for mutants expressing identical amounts of fusion protein, we conclude that the constructs are expressed at low enough concentration that even wild-type fusion protein must be significantly monomeric. It is necessary to assume a wild-type monomer fraction of at least 0.33, and probably ≥ 0.5 , to account for the range of observed CAT activity and to allow direct correlation with the free energy changes measured independently in the ultracentrifuge for the same glycoporphin A mutants.

It is important to understand how the approximation in our derivation affects the value of the apparent association constant K_{app} , from which we calculate $\Delta\Delta G_{app}$. The correct expression for K_a squares $[P_{total}] - 2[P_2]$ in the denominator (equation (3)), but our expression for K_{app} squares a term proportional to $[P_{total}]$. We approximate the fraction of monomer as $[P_{total}]$ because calculating $[P_{total}] - 2[P_2]$ from TOXCAT observable parameters would require coefficients α and β from equations (6) and (7). The effect of this approximation on $\Delta\Delta G_{app}$ is illustrated by the calculated curves in Figure 7. In the dilute limit, where nearly 100% of the wild-type fusion protein is monomeric, $\Delta\Delta G_{app}$ calculated from equation (10) accurately reflects $\Delta\Delta G$ over the entire range. However, if the wild-type construct were only 10% monomeric at the concentrations in the membrane, a true destabilization of 1.0 kcal mol⁻¹ would give $\Delta\Delta G_{app}$ of just 0.08 kcal mol⁻¹ because the fraction of dimer would only drop from 90% to 78%. The concomitant doubling of the fraction of monomer (10% to 22%) is neglected in calculating $\Delta\Delta G_{app}$ due to our approximation. Thus, if the wild-type ToxR'(GpA-TMD)MBP fusion protein

Figure 6. Simulations suggest that the effects of mutations on measured CAT levels are consistent with low fractional dimerization of the wild-type fusion protein. The continuous curves depict how CAT activity (*y*-axis) would drop off as the dimer is destabilized up to 4 kcal mol⁻¹ (*x*-axis) when the wild-type construct is assumed to be present at the indicated mole fractions of monomer; the two unlabeled lines farthest to the left are for wild-type monomer mole fractions of 0.98 and 0.998. CAT activities (yellow bars) for wild-type glycoporphin A and 18 mutants are presented at horizontal positions corresponding to the free energy change for each variant as measured by sedimentation equilibrium.

were primarily dimeric in *E. coli* membranes, the assumption used in calculating $\Delta\Delta G_{app}$ from TOXCAT data would compress the apparent free energy scale, resulting in the slope of a plot of $\Delta\Delta G_{app}$ versus $\Delta\Delta G_{mut}$ being much less than unity. For instance, if the wild-type construct were just 10% monomeric, the slope of a regression line for $\Delta\Delta G_{app}$ versus $\Delta\Delta G$ would be just 0.454 (from a linear fit to the calculated data in Figure 7 over the range 0 to 4 kcal mol⁻¹). Although we cannot directly measure the fractional association of the wild-type fusion protein by our method, the slope of 1.07 for the regression analysis of $\Delta\Delta G_{app}$ versus $\Delta\Delta G_{mut}$ allows us to infer that the wild-type construct must sample the monomeric state substantially.

A weak correlation between $\Delta\Delta G_{app}$ and dimerization phenotypes from SDS-PAGE is improved by a hydrophobicity term

We performed regression analysis between the $\Delta\Delta G_{app}$ values described here and the previously reported dimerization phenotypes for the same mutations in the glycoporphin A TMD under conditions of SDS-PAGE.³³ Based on their dimerization on SDS-PAGE, mutants were previously assigned scores_{SDS}=0 (as wild-type), 1 (significant dimer), 2 (detectable dimer), or 3 (no dimer). Figure 8 shows that $\Delta\Delta G_{app}$ correlates weakly with scores_{SDS} ($R=0.53$, Figure 8(a)), but the agreement can be considerably improved ($R=0.71$, Figure 8(b)) by including a term for the change of hydrophobicity that accompanies the mutation (fitting $\Delta\Delta G_{app}$ versus scores_{SDS} - $\Delta H\Phi$, where $\Delta H\Phi$ is the difference in hydrophobicity between the replacing and original residue on the biological hydrophobicity

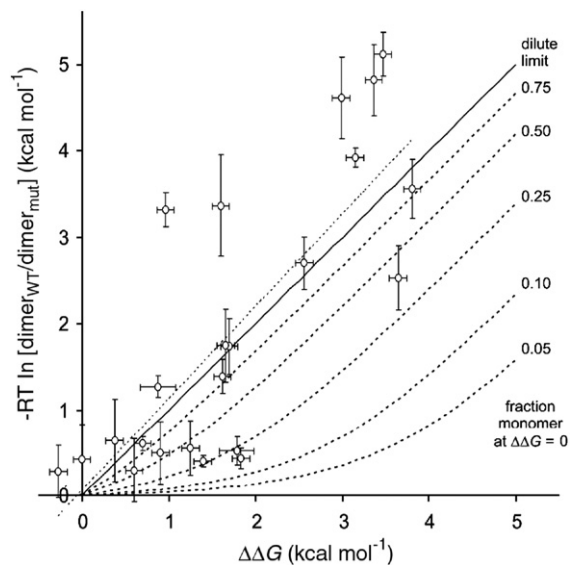


Figure 7. Predicted deviation of $\Delta\Delta G_{app}$ from $\Delta\Delta G$ for varying absolute association of wild-type fusion construct. For wild-type species with the fraction monomeric protein indicated at right, we calculate monomer and dimer fractions exactly for a range of $\Delta\Delta G$ (using K_a from equation (3)) and then calculate $\Delta\Delta G_{app}$ using the first term of equation (10) ($-RT \ln [\text{dimer}_{WT}/\text{dimer}_{mut}]$), which assumes that the mole fraction of monomeric protein can be approximated as the total protein. In the dilute limit (continuous line, slope=1) the assumption holds, but as the fraction of monomeric protein decreases, $\Delta\Delta G_{app}$ initially changes more slowly than $\Delta\Delta G$ (broken lines). The ($\Delta\Delta G_{mut}$, $\Delta\Delta G_{app}$) data points from Figure 5 except mutants at Thr87 have been superimposed along with the linear regression for these points (dotted line, slope=1.08).

scale⁴¹). Omitting the mutants at position Thr87 improves these fits only slightly ($R=0.57$ or 0.75 for Figure 8(a) or (b), respectively).

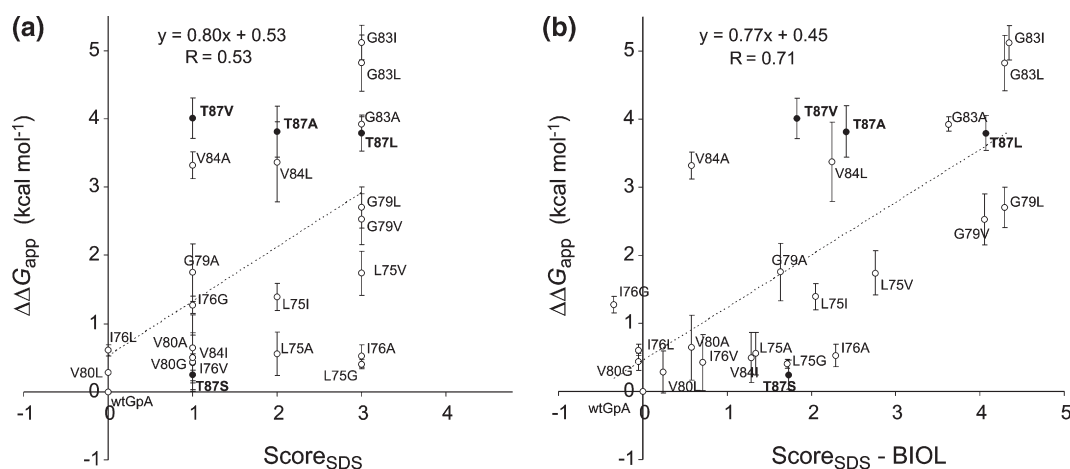


Figure 8. Regression analysis of apparent free energies from TOXCAT versus the SDS-PAGE phenotypes of Lemmon *et al.*³³ The poor fit achieved using the arbitrary scale of the SDS-PAGE phenotypes (a) can be significantly improved by adding a term that accounts for the change in hydrophobicity of each substitution (b). Mutations at Thr87 are presented as black dots.

Discussion

TOXCAT measures changes in association free energy due to mutations

We show here that the TOXCAT assay can be used to measure changes in the apparent free energy of *in vivo* dimerization of a transmembrane domain that result from point mutations. Wild-type and mutant constructs show up to 200-fold differences in reporter gene expression, giving a large dynamic range that compares favorably with the extent of modulation of gene expression observed for the intact ToxR/ctx system^{42,43} upon which the TOXCAT assay is based. Although there is some variation in fusion protein expression levels, the experimental values for $\Delta\Delta G_{app}$ are very reproducible from one culture to the next, and for most mutants $\Delta\Delta G_{app}$ from TOXCAT is quite similar to $\Delta\Delta G_{mut}$ from ultracentrifugation. Despite the approximations made in deriving equation (10) and the complexity of the biological system in which the TOXCAT data are acquired, the near-unity slope for the regression analysis in Figure 5 strongly suggests that the TOXCAT method for determining $\Delta\Delta G_{app}$ agrees closely with ultracentrifugation-derived measures of the effects of mutations on the self-association of the glycoprotein A transmembrane domain. The near-zero intercept of the same regression analysis further suggests that the TOXCAT assay is sensitive to even small decreases in the stability of the glycoprotein A TMD dimer. The similarities between $\Delta\Delta G_{app}$ and $\Delta\Delta G_{mut}$ indicate that the TOXCAT approach can be as quantitative as a biophysical approach to measuring effects of mutagenesis on association, and that sedimentation equilibrium measurements in detergents can accurately report on the same phenomena that occur in membranes of living cells.

The excellent quantitative agreement with the thermodynamic data from detergent micelles may be somewhat surprising, given that the approach described here does not systematically perturb the mole fraction of fusion protein in the membrane, does not measure the fraction of dimeric ToxR fusion protein at all, and therefore does not determine ΔG_{app} . Rather, we extract $\Delta\Delta G_{\text{app}}$ by assuming that the TOXCAT reporter gene expression is proportional to the fraction of dimer and that the total amount of fusion protein is proportional to a Western blot intensity, and then using the ratio of mutant and wild-type values for these two measurables to calculate $\Delta\Delta G_{\text{app}}$ (while assuming that the mole fraction of dimers is small).

Because sequence changes could possibly alter the expression levels or the membrane insertion efficiency of the TOXCAT fusion proteins, we tested our library of mutant constructs for proper topology of membrane insertion and measured the amount of TOXCAT protein in each sample assayed for reporter gene expression. Although we found no evidence of altered membrane insertion, we did observe up to threefold changes in the levels of expressed ToxR fusion protein for mutant proteins compared to wild-type (see distribution in Figure 4). Cells expressing significantly higher levels of a particular fusion protein on a given day also show higher reporter gene expression for that culture. Higher CAT expression for a given sample lowers the reporter gene term $-RT \ln [\text{CAT}_{\text{mut}}/\text{CAT}_{\text{WT}}]$ compared to other replicates, but elevated Western blot intensity increases the fusion protein term $-RT \ln [\text{WB}_{\text{WT}}/\text{WB}_{\text{mut}}]^2$. This compensation is illustrated across our entire data set in Table 1, where we show that combining these two terms to calculate $\Delta\Delta G_{\text{app}}$ for each replicate experiment before averaging gives a much smaller standard error than averaging the triplicates for each term and then combining them to calculate $\Delta\Delta G_{\text{app}}$. Thus, although our approach does not systematically alter the level of ToxR fusion protein expression in cells, we do observe the expected trends in the observables when fusion protein levels vary stochastically. The compensations between the terms in equation (10) that result in good agreement between independent replicate measurements of $\Delta\Delta G_{\text{app}}$ suggest that our data are reporting on equilibrium association of the ToxR fusion protein in cell membranes.

The role of Thr87 in glycoporphin A dimerization depends on the lipidic environment

Despite generally good agreement between the $\Delta\Delta G_{\text{app}}$ values reported here and the $\Delta\Delta G_{\text{mut}}$ measurements by Fleming and colleagues, there are statistically significant differences between these observations for eight single point mutants, including three outliers that map to Thr87 and that are all more disruptive *in vivo* than *in vitro*. The TOXCAT data show that all four apolar substitutions at Thr87 are strongly disruptive whereas Thr87Ser is essentially non-disruptive. Together,

these data suggest that the polar side-chain γ oxygen of Thr87 is critical for dimerization, particularly since isosteric Thr87Val is strongly disruptive, but Thr87Ser (which retains the side-chain γ oxygen) permits wild-type association. The ultracentrifugation data, on the other hand, show a graded disruptive effect for mutations at position Thr87, with the rank order of disruption correlating with size (Leu > Ile > Val > Ala ~ Ser). Because Val is more disruptive than Ser, a role for the side-chain γ oxygen might be inferred, but Ala is as mildly disruptive as Ser, implying that a small residue can suffice at this position. The solution NMR structure of glycoporphin A in detergent micelles indicates that the Thr87 side-chain donates a hydrogen bond to the carbonyl oxygen of Gly83 of the same helix and packs with the opposite monomer.⁴⁴ However, solid state NMR experiments on glycoporphin A peptides reconstituted into lipid bilayers suggest that the side-chain of Thr87 could be involved in an intermonomer hydrogen bond.⁴⁵ The discrepancies between $\Delta\Delta G_{\text{app}}$ and $\Delta\Delta G_{\text{mut}}$ for mutations at Thr87 may therefore reflect differences in the structure of the glycoporphin A dimer interface in bilayers compared to detergent micelles. Another possibility is that Thr87 (and variants) could contribute differentially to stability in detergents compared to membranes through effects on the free energy of the monomeric state.

Hydrophobicity changes influence dimerization in SDS but not in membranes

Although $\Delta\Delta G_{\text{app}}$ achieves only weak agreement with the qualitative dimerization phenotypes reported based on SDS-PAGE assays, the agreement can be substantially improved by including a term that modifies the SDS-PAGE score by the difference in hydrophobicity caused by the mutation (see Figure 8). This suggests that loss of hydrophobicity within the transmembrane domain of glycoporphin A decreases dimer stability under conditions of SDS-PAGE but does not affect dimer stability as measured by TOXCAT. Russ and Engelman drew a similar conclusion from the observation that tyrosine substitutions at non-interfacial positions of the glycoporphin A TMD are non-disruptive in TOXCAT but disruptive on SDS-PAGE.¹⁴ The relative hydrophobicity of mutations also affects the self-association of the BNIP3 TMD in SDS-PAGE: hydrophobic substitutions away from the dimer interface have little or no effect on dimerization, while polar substitutions are generally disruptive.⁴⁶ The results presented here support the proposal⁴⁶ that polar substitutions affect the apparent stability of TMD interactions by causing the TMD to unfold in a detergent environment, allowing it to access a conformation that would not be available in the two-stage model for membrane protein folding in a bilayer.⁴⁷ The influence of hydrophobicity on the helicity of peptides in lipidic environments is well known⁴⁸ and has been proposed to result from coupling between partitioning and folding.⁴⁹ By

showing that quantitative agreement between *in vivo* and SDS-PAGE assays for self-association can be improved using a term for hydrophobicity, the present work suggests that under some conditions hydrophobic partitioning can be coupled to helix–helix association, as predicted by the interface-centered membrane protein folding thermodynamic formalism described by White and Wimley.⁴⁹ This is also supported by findings from the BNIP3 system in which decreases in hydrophobicity cause loss of helicity and enhance backbone amide exchange.⁴⁶ Therefore, although SDS micelles act as a poor membrane mimetic for some transmembrane spans, it may be possible to use appropriate hydrophobicity or partitioning scales^{41,50,51} to “correct” results from this detergent to better reflect the results obtained in membranes. Minimal improvements are achieved when a similar correction is attempted for the regression analysis of $\Delta\Delta G_{\text{app}}$ and $\Delta\Delta G_{\text{mut}}$, suggesting that the detergent used for the ultracentrifugation analysis (C_8E_5) is a better membrane mimetic than SDS. We note, however, that the three most N-terminal outliers from the *t*-test comparison of $\Delta\Delta G_{\text{app}}$ and $\Delta\Delta G_{\text{mut}}$ (Leu75Gly, Ile76Ala, and Val80Gly) represent large-to-small mutations that are more disruptive in the ultracentrifuge than in TOXCAT; for these substitutions, hydrophobicity changes would be expected to contribute substantially to the discrepancy between the TOXCAT data and the ultracentrifugation data.

Validity of the assumption that the fusion protein is largely monomeric

The theoretical basis for our approach includes the assumption that the amount of monomeric fusion protein in the cell membrane can be approximated as the amount of total protein ($[P] \approx [P_{\text{total}}]$, equation (4)). Although we have no direct measures of the fractional association of the wild-type ToxR'(GpA-TMD)MBP fusion protein, a comparison of theoretical association curves with the range of observed CAT activities plotted against $\Delta\Delta G_{\text{mut}}$ (Figure 6) strongly suggests that the fusion protein is expressed at mole fractions low enough to keep it largely monomeric. Substantial deviation from a linear fit with a slope of unity would have been expected for a regression analysis of $\Delta\Delta G_{\text{app}}$ versus $\Delta\Delta G_{\text{mut}}$ (Figure 7) if the wild-type fusion protein were present at high mole fractions, causing it to be overwhelmingly dimeric. No such trends appear in our data: $\Delta\Delta G_{\text{app}}$ and $\Delta\Delta G_{\text{mut}}$ data pairs are statistically indistinguishable for more than 70% of the mutants by Student's *t*-test, and the near-unity slope of the regression analysis in Figure 5 shows clearly that the scale of $\Delta\Delta G_{\text{app}}$ is not compressed compared to that of $\Delta\Delta G_{\text{mut}}$. The calculated curves in Figure 7 indicate that the deviation of $\Delta\Delta G_{\text{app}}$ from $\Delta\Delta G_{\text{mut}}$ would not drown out the correlation even at just 25% monomer, and so we suggest that TOXCAT should be able to differentiate between dimerization of the wild-type glycoporphin A transmembrane domain and species that associate even

more tightly. If, however, the fusion protein were to be expressed at much higher levels, or if the sequence under study were to have a significantly tighter association constant, it would be possible to enter a regime where sequence changes had little effect on TOXCAT signals, and the apparent free energy scale would be compressed.

The strong homodimerization of the glycoporphin A transmembrane domain has made it a positive control for biological assays of transmembrane helix–helix interactions, but measurements of the fractional association of membrane-inserted glycoporphin A fusion proteins *in vivo* have not been obtained until recently. Schneider and colleagues varied the expression level of wild-type and mutant glycoporphin A GALLEX fusion proteins in cells with an inducible promoter and used the saturation of the GALLEX signal to estimate the concentration at which reporter gene expression is 50% repressed.⁵² Since the GALLEX and TOXCAT fusions are presumably expressed at different levels, and must have different free energy contributions to dimerization from extramembraneous protein–protein interactions and from protein–nucleic acid interactions, the fractional association of fusion proteins for these two systems would not be expected to be the same. However, Schneider and colleagues used wild-type and mutant ΔG_{dimer} measurements to calculate $\Delta\Delta G_{\text{mut}}$ values for five mutants that we have analyzed here using TOXCAT. Table 2 presents the analytical ultracentrifugation, GALLEX, and TOXCAT data for these five point mutants. The rank order of stability of these mutants is roughly conserved in the three assays, but the free energy scale for the GALLEX measurements appears to be more compressed than the TOXCAT or sedimentation equilibrium data.

The method presented here measures the effects of point mutations on the free energy of helix–helix interactions within membranes of living cells. Given the many components in the cell membrane and the number of biological processes and biochemical procedures upon which TOXCAT depends, it is remarkable that the TOXCAT approach achieves the present level of agreement with thermodynamic data from biophysical measurements on purified

Table 2. Changes in association free energy for five glycoporphin A mutants from ultracentrifugation and two biological assays

	$\Delta\Delta G_{\text{AU}}$ (kcal mol ⁻¹)	$\Delta\Delta G_{\text{GALLEX}}$ (kcal mol ⁻¹)	$\Delta\Delta G_{\text{TOXCAT}}$ (kcal mol ⁻¹)
Leu75Val	1.7	0.23	1.74
Gly79Ala	1.7	1.20	1.75
Gly79Ile	3.0	1.61	4.61
Gly83Ala	3.1	1.00	3.92
Gly83Ile	3.5	2.15	5.11

$\Delta\Delta G_{\text{AU}}$ data are from Fleming & Engelman,⁸ and Doura et al.;¹⁰ errors are 0.1–0.2 kcal mol⁻¹.

$\Delta\Delta G_{\text{GALLEX}}$ data are from Finger et al.⁵²

$\Delta\Delta G_{\text{TOXCAT}}$ data are from the present work; errors are 0.1–0.5 kcal mol⁻¹.

proteins. Although we measure only an apparent change in the free energy of helix–helix interaction, the internal consistency of our findings, the compensation between the terms $-RT \ln [\text{CAT}_{\text{mut}}/\text{CAT}_{\text{WT}}]$ and $-RT \ln [\text{WB}_{\text{WT}}/\text{WB}_{\text{mut}}]^2$, and the agreement with genuine thermodynamic data suggest that the TOXCAT system is actually providing a thermodynamic read-out of transmembrane domain dimerization. These results demonstrate that complex biological processes (transcription of a reporter gene) can be regulated by the stability of helix–helix association in membranes and that the thermodynamic effects of single point mutations as measured in detergents can accurately predict the effects of these mutations in complex biological systems. We expect that the combination of thermodynamic measurements on purified proteins in detergents and in bilayers as well as the characterization of interactions using TOXCAT or other biological assays will be critical to the continued development of insights into the specificity and stability of transmembrane domain interactions.

Experimental Methods

Constructs and site-directed mutagenesis

The pccKAN vector expressing a ToxR'(GpA-TMD)MBP chimera was described previously by Russ and Engelman.¹⁴ Single-point mutations within the wild-type glycoporphin A TMD were generated using the QuikChange kit (Stratagene, La Jolla, CA), and mutations were confirmed by automated dideoxynucleotide sequencing.

TOXCAT cultures

All media contained 50 $\mu\text{g ml}^{-1}$ carbenicillin. Plasmids containing wild-type and mutant pccKToxR'(GpA-TMD)MBP chimerae were transformed into *E. coli* NT326 cells and plated on Luria Bertani (LB) plates. Colonies were grown in LB medium until $A_{420} \sim 0.2$, and then stored as glycerol stocks at -80°C . LB cultures were inoculated from glycerol stocks and grown at 37°C overnight. 40 μl of overnight culture was diluted into fresh LB culture tubes, grown until $A_{420} \sim 1.0$, and 10.0 A_{420} units of cells were harvested by centrifugation at 13,000g for 5 min. (Note that when studying the BNIP3 TMD, we harvested 4.0 A_{420} units of cells³⁸). The cell pellets were washed with 0.4 ml of sonication buffer (25 mM Tris-HCl, 2 mM EDTA, pH 8.0) and resuspended in 2 ml of sonication buffer for lysis by probe sonication. After removing an aliquot of the whole cell lysate for Western blot analysis, the remaining lysate was centrifuged at 13,000g for 15 min, and the supernatant (cleared lysate) was stored at -20°C for spectrophotometric CAT assay.

Spectrophotometric CAT assay

The method described by Shaw³⁷ was used to measure CAT activity in cleared cell lysates. The rate of transfer of an acetyl group from acetyl-CoA to chloramphenicol is detected by the rate of color change (412 nm) associated with the reaction of the resulting free coenzyme A with

5,5'-dithiobis-(2-nitrobenzoic acid) (DTNB). 12 μl of cleared lysate was mixed with 300 μl reaction buffer (0.1 mM acetyl-CoA, 0.4 mg/ml DTNB, 0.1 M Tris-HCl, pH 7.8) and the absorbance at 412 nm was measured on a Cary 50 spectrophotometer at 3 s intervals for 2 min to obtain the background rate of acetyl-CoA hydrolysis. 12 μl of 2.5 mM chloramphenicol was then added to the reaction, mixed thoroughly, and the absorbance at 412 nm was again measured for 1 min; for samples that showed very low levels of CAT activity, the measuring time was extended to 2 min. Each lysate was assayed in triplicate, and the average change in absorbance at 412 nm was converted into CAT enzyme activity ($\epsilon=13,600$).

Western blots

Aliquots of whole cell lysate were brought to 0.1 mg ml^{-1} hen egg white lysozyme and incubated on ice for 15 min. 0.01 unit of DNase I was added to the reaction and incubated on ice for a further 20 min. Samples were mixed with equal volumes of 2 \times SDS-PAGE sample buffer (with 0.1 M dithiothreitol), heated to 95°C for 10 min, separated on pre-cast 15% (w/v) polyacrylamide gels (Bio-Rad), blotted onto nitrocellulose membranes, and blocked in skim milk. ToxR'(GpA-TMD)MBP chimera were detected with biotinylated anti-MBP primary antibody and visualized with streptavidin-horseradish peroxidase conjugate and ECL reagent (Amersham Biosciences). An Alpha Innotech digital camera system (equipped with a cooled CCD) was used to image the membranes and measure the intensities of the bands.

Maltose complementation assay

E. coli NT326 cultures carrying the ToxR'(GpA-TMD)MBP constructs were inoculated from glycerol stocks into LB and grown at 37°C overnight. 10 μl of overnight culture was added to fresh culture tubes containing M9 minimal medium (0.4% (w/v) glucose as sole carbon source), grown at 37°C for 8 h, streaked on M9 minimal media plates containing 0.4% maltose as sole carbon source, and incubated at 37°C for three days. Plates were imaged using an Alpha Innotech digital camera system.

Apparent free energy difference calculations

The apparent change in free energy of association for a mutant transmembrane domain relative to the wild-type transmembrane domain is given by $\Delta\Delta G_{\text{app}} = -RT \ln K_{\text{app}}$ where:

$$K_{\text{app}} = \frac{\text{CAT}_{\text{mut}} (\text{WB}_{\text{WT}})^2}{\text{CAT}_{\text{WT}} (\text{WB}_{\text{mut}})^2}$$

CAT_{mut} and CAT_{WT} are the chloramphenicol acetyl transferase activities of mutant and wild-type lysates, and WB_{WT} and WB_{mut} are the Western blot band intensities (in arbitrary units) for full-length wild-type and mutant ToxR'(GpA-TMD)MBP chimerae. Reported values for $\Delta\Delta G_{\text{app}}$ are the mean (\pm standard deviation) of three independent experiments. Values for $\Delta\Delta G_{\text{app}}$ are reported to the second decimal place in Table 1 to clarify the calculation of standard deviations; the average precision for these measured values is about 0.3 kcal mol^{-1} (based on triplicate independent cultures), and precisions for individual mutants range from 0.1 to 0.5 kcal mol^{-1} (see column $\text{SD}_{\Delta\Delta G}$ in Table 1).

Statistical analyses

Values for $\Delta\Delta G_{\text{app}}$ (from TOXCAT; Table 1) and $\Delta\Delta G_{\text{mut}}$ (from ultracentrifugation^{2,8,10}) were compared using a Student's *t*-test (two degrees of freedom) to determine the significance of differences in the measurements. For the TOXCAT data, the standard deviation used was the higher of $SD_{\Delta\Delta G}$ from Table 1 or 0.2 kcal mol⁻¹. The standard deviations used for the ultracentrifugation data were from the cited literature,^{2,8,10} and were typically 0.1 or 0.2 kcal mol⁻¹.

Acknowledgements

We thank J.S. Olson for comments and criticism on the experiments, the analysis, and the manuscript. This work was supported by Robert A. Welch Foundation grant C-1513 (to K.R.M.), NIH grant R01 GM067850 (to K.R.M.), and by NSF grant MCB0423807 (to K.G.F.). TMJ was supported by an NIH Molecular Biophysics Training Grant (T32 GM008280).

References

- MacKenzie, K. R. (2006). Folding and stability of alpha-helical integral membrane proteins. *Chem. Rev.* **106**, 1931–1977.
- Fleming, K. G., Ackerman, A. L. & Engelman, D. M. (1997). The effect of point mutations on the free energy of transmembrane alpha-helix dimerization. *J. Mol. Biol.* **272**, 266–275.
- Fleming, K. G. (2000). Probing stability of helical transmembrane proteins. *Methods Enzymol.* **323**, 63–77.
- Fleming, K. G. (2002). Standardizing the free energy change of transmembrane helix-helix interactions. *J. Mol. Biol.* **323**, 563–571.
- Cristian, L., Lear, J. D. & DeGrado, W. F. (2003). Determination of membrane protein stability via thermodynamic coupling of folding to thiol-disulfide interchange. *Protein Sci.* **12**, 1732–1740.
- Cristian, L., Lear, J. D. & DeGrado, W. F. (2003). Use of thiol-disulfide equilibria to measure the energetics of assembly of transmembrane helices in phospholipid bilayers. *Proc. Natl Acad. Sci. USA*, **100**, 14772–14777.
- You, M., Li, E., Wimley, W. C. & Hristova, K. (2005). Forster resonance energy transfer in liposomes: measurements of transmembrane helix dimerization in the native bilayer environment. *Anal. Biochem.* **340**, 154–164.
- Fleming, K. G. & Engelman, D. M. (2001). Specificity in transmembrane helix-helix interactions can define a hierarchy of stability for sequence variants. *Proc. Natl Acad. Sci. USA*, **98**, 14340–14344.
- Doura, A. K. & Fleming, K. G. (2004). Complex interactions at the helix-helix interface stabilize the glycoporphin A transmembrane dimer. *J. Mol. Biol.* **343**, 1487–1497.
- Doura, A. K., Kobus, F. J., Dubrovsky, L., Hibbard, E. & Fleming, K. G. (2004). Sequence context modulates the stability of a GxxxG-mediated transmembrane helix-helix dimer. *J. Mol. Biol.* **341**, 991–998.
- Stouffer, A. L., Nanda, V., Lear, J. D. & DeGrado, W. F. (2005). Sequence determinants of a transmembrane proton channel: an inverse relationship between stability and function. *J. Mol. Biol.* **347**, 169–179.
- Langosch, D., Brosig, B., Kolmar, H. & Fritz, H. J. (1996). Dimerisation of the glycoporphin A transmembrane segment in membranes probed with the ToxR transcription activator. *J. Mol. Biol.* **263**, 525–530.
- Brosig, B. & Langosch, D. (1998). The dimerization motif of the glycoporphin A transmembrane segment in membranes: importance of glycine residues. *Protein Sci.* **7**, 1052–1056.
- Russ, W. P. & Engelman, D. M. (1999). TOXCAT: a measure of transmembrane helix association in a biological membrane. *Proc. Natl Acad. Sci. USA*, **96**, 863–868.
- Leeds, J. A., Boyd, D., Huber, D. R., Sonoda, G. K., Luu, H. T., Engelman, D. M. & Beckwith, J. (2001). Genetic selection for and molecular dynamic modeling of a protein transmembrane domain multimerization motif from a random *Escherichia coli* genomic library. *J. Mol. Biol.* **313**, 181–195.
- Gurezka, R. & Langosch, D. (2001). In vitro selection of membrane-spanning leucine zipper protein-protein interaction motifs using POSSYCCAT. *J. Biol. Chem.* **276**, 45580–45587.
- Schneider, D. & Engelman, D. M. (2003). GALLEX, a measurement of heterologous association of transmembrane helices in a biological membrane. *J. Biol. Chem.* **278**, 3105–3111.
- Laage, R. & Langosch, D. (1997). Dimerization of the synaptic vesicle protein synaptobrevin (vesicle-associated membrane protein) II depends on specific residues within the transmembrane segment. *Eur. J. Biochem.* **249**, 540–546.
- Gurezka, R., Laage, R., Brosig, B. & Langosch, D. (1999). A heptad motif of leucine residues found in membrane proteins can drive self-assembly of artificial transmembrane segments. *J. Biol. Chem.* **274**, 9265–9270.
- Laage, R., Rohde, J., Brosig, B. & Langosch, D. (2000). A conserved membrane-spanning amino acid motif drives homomeric and supports heteromeric assembly of presynaptic SNARE proteins. *J. Biol. Chem.* **275**, 17481–17487.
- Mendrola, J. M., Berger, M. B., King, M. C. & Lemmon, M. A. (2002). The single transmembrane domains of ErbB receptors self-associate in cell membranes. *J. Biol. Chem.* **277**, 4704–4712.
- Bowen, M. E., Engelman, D. M. & Brunger, A. T. (2002). Mutational analysis of synaptobrevin transmembrane domain oligomerization. *Biochemistry*, **41**, 15861–15866.
- McClain, M. S., Iwamoto, H., Cao, P., Vinion-Dubiel, A. D., Li, Y., Szabo, G., Shao, Z. & Cover, T. L. (2003). Essential role of a GXXXG motif for membrane channel formation by *Helicobacter pylori* vacuolating toxin. *J. Biol. Chem.* **278**, 12101–12108.
- Roy, R., Laage, R. & Langosch, D. (2004). Synaptobrevin transmembrane domain dimerization-revisited. *Biochemistry*, **43**, 4964–4970.
- Ruan, W., Lindner, E. & Langosch, D. (2004). The interface of a membrane-spanning leucine zipper mapped by asparagine-scanning mutagenesis. *Protein Sci.* **13**, 555–559.
- Melnyk, R. A., Kim, S., Curran, A. R., Engelman, D. M., Bowie, J. U. & Deber, C. M. (2004). The affinity of GXXXG motifs in transmembrane helix-helix interactions is modulated by long-range communication. *J. Biol. Chem.* **279**, 16591–16597.

27. Schneider, D. & Engelman, D. M. (2004). Motifs of two small residues can assist but are not sufficient to mediate transmembrane helix interactions. *J. Mol. Biol.* **343**, 799–804.
28. Schneider, D. & Engelman, D. M. (2004). Involvement of transmembrane domain interactions in signal transduction by alpha/beta integrins. *J. Biol. Chem.* **279**, 9840–9846.
29. Li, R., Gorelik, R., Nanda, V., Law, P. B., Lear, J. D., DeGrado, W. F. & Bennett, J. S. (2004). Dimerization of the transmembrane domain of Integrin alphaIIb subunit in cell membranes. *J. Biol. Chem.* **279**, 26666–26673.
30. Chin, C. N., Sachs, J. N. & Engelman, D. M. (2005). Transmembrane homodimerization of receptor-like protein tyrosine phosphatases. *FEBS Letters*, **579**, 3855–3858.
31. Zhou, F. X., Merianos, H. J., Brunger, A. T. & Engelman, D. M. (2001). Polar residues drive association of polyleucine transmembrane helices. *Proc. Natl Acad. Sci. USA*, **98**, 2250–2255.
32. Zhou, F. X., Cocco, M. J., Russ, W. P., Brunger, A. T. & Engelman, D. M. (2000). Interhelical hydrogen bonding drives strong interactions in membrane proteins. *Nature Struct. Biol.* **7**, 154–160.
33. Lemmon, M. A., Flanagan, J. M., Hunt, J. F., Adair, B. D., Bormann, B. J., Dempsey, C. E. & Engelman, D. M. (1992). Glycophorin A dimerization is driven by specific interactions between transmembrane alpha-helices. *J. Biol. Chem.* **267**, 7683–7689.
34. Lemmon, M. A., Treutlein, H. R., Adams, P. D., Brunger, A. T. & Engelman, D. M. (1994). A dimerization motif for transmembrane alpha-helices. *Nature Struct. Biol.* **1**, 157–163.
35. Fleming, K. G., Ren, C. C., Doura, A. K., Easley, M. E., Kobus, F. J. & Stanley, A. M. (2004). Thermodynamics of glycophorin A transmembrane helix dimerization in C14 betaine micelles. *Biophys. Chem.* **108**, 43–49.
36. Lemmon, M. A., Flanagan, J. M., Treutlein, H. R., Zhang, J. & Engelman, D. M. (1992). Sequence specificity in the dimerization of transmembrane alpha-helices. *Biochemistry*, **31**, 12719–12725.
37. Shaw, W. V. (1975). Chloramphenicol acetyltransferase from chloramphenicol-resistant bacteria. *Methods Enzymol.* **43**, 737–755.
38. Sulistijo, E. S., Jaszewski, T. M. & MacKenzie, K. R. (2003). Sequence-specific dimerization of the transmembrane domain of the “BH3-only” protein BNIP3 in membranes and detergent. *J. Biol. Chem.* **278**, 51950–51956.
39. Gorman, C. M., Moffat, L. F. & Howard, B. H. (1982). Recombinant genomes which express chloramphenicol acetyltransferase in mammalian cells. *Mol. Cell. Biol.* **2**, 1044–1051.
40. Young, S. L., Barbera, L., Kaynard, A. H., Haugland, R. P., Kang, H. C., Brinkley, M. & Melner, M. H. (1991). A nonradioactive assay for transfected chloramphenicol acetyltransferase activity using fluorescent substrates. *Anal. Biochem.* **197**, 401–407.
41. Hessa, T., Kim, H., Bihlmaier, K., Lundin, C., Boekel, J., Andersson, H. *et al.* (2005). Recognition of transmembrane helices by the endoplasmic reticulum translocon. *Nature*, **433**, 377–381.
42. Miller, V. L. & Mekalanos, J. J. (1984). Synthesis of cholera toxin is positively regulated at the transcriptional level by toxR. *Proc. Natl Acad. Sci. USA*, **81**, 3471–3475.
43. Miller, V. L., Taylor, R. K. & Mekalanos, J. J. (1987). Cholera toxin transcriptional activator toxR is a transmembrane DNA binding protein. *Cell*, **48**, 271–279.
44. MacKenzie, K. R., Prestegard, J. H. & Engelman, D. M. (1997). A transmembrane helix dimer: structure and implications. *Science*, **276**, 131–133.
45. Smith, S. O., Eilers, M., Song, D., Crocker, E., Ying, W., Groesbeck, M. *et al.* (2002). Implications of threonine hydrogen bonding in the glycophorin A transmembrane helix dimer. *Biophys. J.* **82**, 2476–2486.
46. Sulistijo, E. S. & Mackenzie, K. R. (2006). Sequence dependence of BNIP3 transmembrane domain dimerization implicates side-chain hydrogen bonding and a tandem GxxxG motif in specific helix-helix interactions. *J. Mol. Biol.* **364**, 974–990.
47. Popot, J. L. & Engelman, D. M. (1990). Membrane protein folding and oligomerization: the two-stage model. *Biochemistry*, **29**, 4031–4037.
48. Li, S. C. & Deber, C. M. (1994). A measure of helical propensity for amino acids in membrane environments. *Nature Struct. Biol.* **1**, 558.
49. White, S. H. & Wimley, W. C. (1998). Hydrophobic interactions of peptides with membrane interfaces. *Biochim. Biophys. Acta*, **1376**, 339–352.
50. Wimley, W. C. & White, S. H. (1996). Experimentally determined hydrophobicity scale for proteins at membrane interfaces. *Nature Struct. Biol.* **3**, 842–848.
51. Wimley, W. C., Creamer, T. P. & White, S. H. (1996). Solvation energies of amino acid side chains and backbone in a family of host-guest pentapeptides. *Biochemistry*, **35**, 5109–5124.
52. Finger, C., Volkmer, T., Prodhon, A., Otzen, D. E., Engelman, D. M. & Schneider, D. (2006). The stability of transmembrane helix interactions measured in a biological membrane. *J. Mol. Biol.* **358**, 1221–1228.

Edited by J. Bowie

(Received 17 December 2006; received in revised form 6 May 2007; accepted 9 May 2007)

Available online 18 May 2007